

# Bipolar Al/O<sub>2</sub> battery with planar electrodes in alkaline and acidic electrolytes

M. ROTA, Ch. COMNINELLIS

*Swiss Federal Institute of Technology, Lausanne, CH-1015, Switzerland*

S. MÜLLER, F. HOLZER, O. HAAS

*Paul Scherrer Institute, Villigen PSI, CH-5232, Switzerland*

Received 18 April 1994; revised 18 July 1994

A filter-press-type Al/O<sub>2</sub> battery with bipolar assembly of the electrodes was developed. The current–voltage curves and power output of monopolar and of bipolar batteries containing one to four cells were measured in alkaline (4 M NaOH and 7.5 M KOH) and acidic (3 M H<sub>2</sub>SO<sub>4</sub> + 0.04 M HCl) electrolytes. The unit cell had an open circuit voltage of 1.85 V in alkaline media and 1.3 V in acidic media. The single bipolar unit delivered a maximum power of about 7.5 W (75 mW cm<sup>-2</sup>) at 0.7 V. The stack (four cells) had a maximum power of 30 W in 4 M NaOH and 35 W in 3 M H<sub>2</sub>SO<sub>4</sub> + 0.04 M HCl. The power output of the bipolar stack determined experimentally for different external loads could be described using the model of an electric equivalent circuit.

## 1. Introduction

Aluminium/air batteries are power sources with a very attractive energy density. From the time when Zaromb [1] suggested Al/air batteries as a power source for electric vehicles, their development has been mainly oriented toward this application, but stationary applications have been envisaged as well. The status of Al/air battery development has been reviewed by Despić [2], Cooper [3] and Scamans [4]. The main components of the battery: aluminium electrode, oxygen electrode and suitable electrolyte systems, have been studied extensively. These studies led to a better understanding of the electrochemistry of aluminium in alkaline, acidic and neutral aqueous electrolytes. Many attempts were made to activate the anodic oxidation of aluminium while reducing aluminium corrosion using alloying elements [5–14] such as Ga, In, Tl, Mg, Mn, Sn, Zn or electrolyte additives like Sn, Ga, In and Zn ions. A major problem is the electrolyte management during operation of the Al/air battery. In order to increase the energy density, a precipitation process to separate the reaction product (Al(OH)<sub>3</sub>) from the alkaline electrolyte was developed and demonstrated [15]. Battery modules with several unit cells have been constructed and tested [16–19]. In the most frequent configuration an anode was sandwiched between two air cathodes [18, 19]. With this arrangement the consumption of the anode is accompanied by an increase of the internal resistance. To avoid this, a special battery with wedge-shaped anodes was designed by Despić [20]. With this renewable anode, the interelectrode distance could be kept constant during operation. In all the experiments reported with this configuration, the unit cells were

electrically connected in series. A more compact battery design is the bipolar arrangement of the cells. Such a configuration has been mentioned in some papers for the Al/O<sub>2</sub> system, but few details were given concerning either the construction of the cells or the results obtained [20–22]. The main advantages of this configuration are a low electrical resistance for the electrode connections and a compact design of the battery with a high surface area per unit volume. Despite its undeniable advantages, the bipolar configuration is not yet frequently encountered in electrochemical power sources. The construction of a bipolar cell is difficult, particularly when one of the electrodes is a porous gas electrode and the other a dimensionally unstable metal electrode.

This paper describes a multicell Al/O<sub>2</sub> battery with planar bipolar electrodes having a total working area of 100 cm<sup>2</sup> for each electrode.

## 2. Experimental details

### 2.1. Battery design

**2.1.1. Single cell configuration.** The battery was built with the configuration of a filter press. The main components of a single cell were the Al-anode, the oxygen cathode and the PVC frame which defines the electrolyte space and guides the electrolyte flow between the anode and the cathode (Fig. 1). The cathode support was an aluminium plate (160 mm × 140 mm × 15 mm) having a cavity (100 mm × 100 mm × 10 mm) filled with synthetic screen (Propyltex<sup>®</sup>) to improve the mechanical stability of the oxygen electrode. Oxygen was supplied through the screen and support body; the latter was

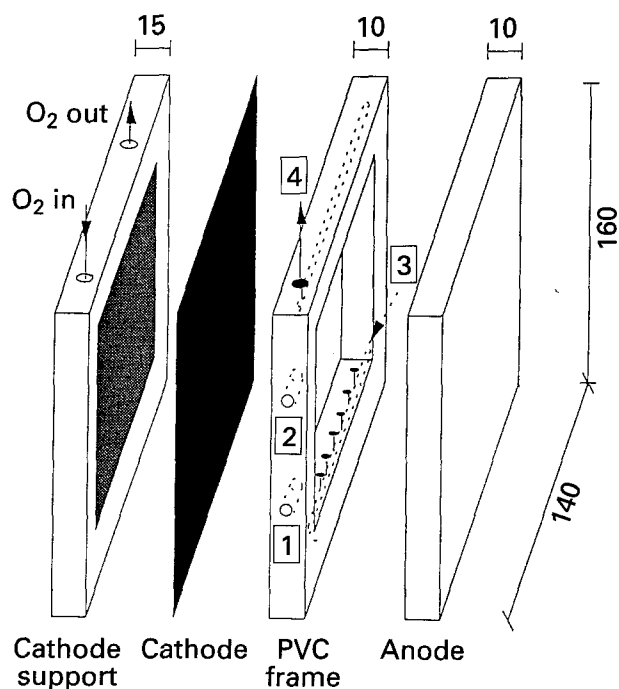


Fig. 1. Construction of a single Al/O<sub>2</sub> cell (dimensions in millimetre). (1) Hole for the reference electrode, (2) hole for the thermocouple, (3) electrolyte inlet, (4) electrolyte outlet. Active surface area of a single electrode: 100 cm<sup>2</sup>.

also used as the current collector. The PVC frame had an array of holes in its lower and upper part for the electrolyte inlet and outlet. Two holes were also pierced through the PVC frame in order to introduce a reference electrode and a thermocouple into the space between the two electrodes. The active electrode area was 100 cm<sup>2</sup> and the interelectrode gap was 10 mm.

The electrolyte in the cell was circulated by an external peristaltic pump (80 ml min<sup>-1</sup>) and passed through a reservoir (0.5 dm<sup>3</sup>) which was kept at constant

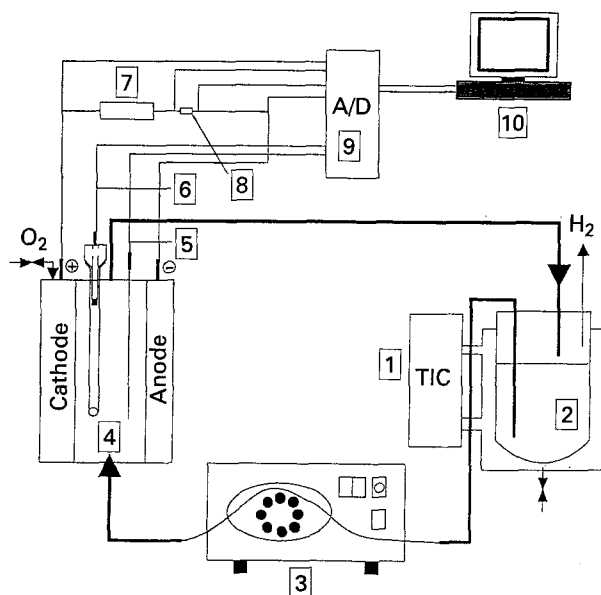


Fig. 2. Schematic view of the experimental setup. (1) Thermostat, (2) reservoir, (3) peristaltic pump, (4) Al/O<sub>2</sub> battery, (5) thermocouple, (6) reference electrode, (7) external resistance, (8) shunt (current measurement), (9) acquisition board, (10) computer.

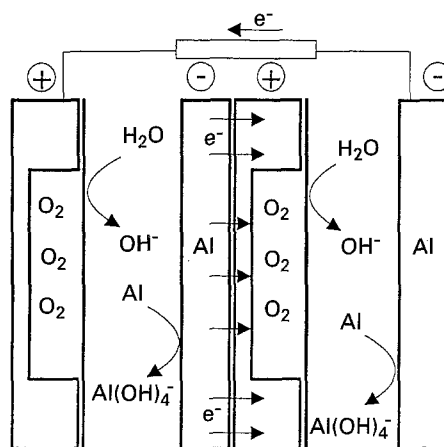


Fig. 3. Schematic representation of a bipolar Al/O<sub>2</sub> battery with two elements.

temperature by a thermostat. This reservoir also functioned as a gas/liquid separator to remove the hydrogen formed by aluminium corrosion (Fig. 2).

Electric connections from both electrodes to the external circuit were achieved by screws penetrating directly the cathode support and the aluminium anode. Electrolyte leakage from the cells was avoided by placing an O-ring on each side of the PVC frame.

**2.1.2. Bipolar configuration.** The bipolar stack design for the Al/O<sub>2</sub> battery is represented in Fig. 3. Anodes and cathodes were clamped together with a PVC frame and the cathode support to constitute the aluminium/oxygen cells in the bipolar arrangement. A configuration with two cells was obtained by placing a bipolar aluminium/oxygen electrode between the oxygen and aluminium electrodes. Only the two end plates of the outer electrodes were connected to the external load. A battery containing up to four cells was also studied. Shunt currents were avoided by using separate electrolyte circuits.

## 2.2. Materials

**2.2.1. Cathodes.** The porous Teflon<sup>®</sup>-bonded O<sub>2</sub>-electrodes were purchased from Eltech Corp. 4 mg cm<sup>-2</sup> of platinum was dispersed in the carbon layer as the catalyst for oxygen reduction. The current collector was a gold-plated silver screen pressed against the gas side of the electrode. The 1.5 mm thick electrodes (140 mm × 140 mm) had an active area of 100 cm<sup>2</sup>. Pure oxygen (99.995%, Carbagas) was supplied in excess.

**2.2.2. Anodes.** The anode materials were kindly provided by Alusuisse-Lonza Service AG. The 10 mm aluminium plates were mechanically polished before use. Four different aluminium alloys were used [13]: Al 99.99%, Al-In 0.05, Al-Zn 6.3Sn 0.16 and Al-In 0.018 Zn 3.2.

**2.2.3. Electrolytes.** NaOH (purum, Fluka), KOH (puriss, Fluka) and H<sub>2</sub>SO<sub>4</sub> (purum, Fluka) were used as received. The electrolyte conductivity at

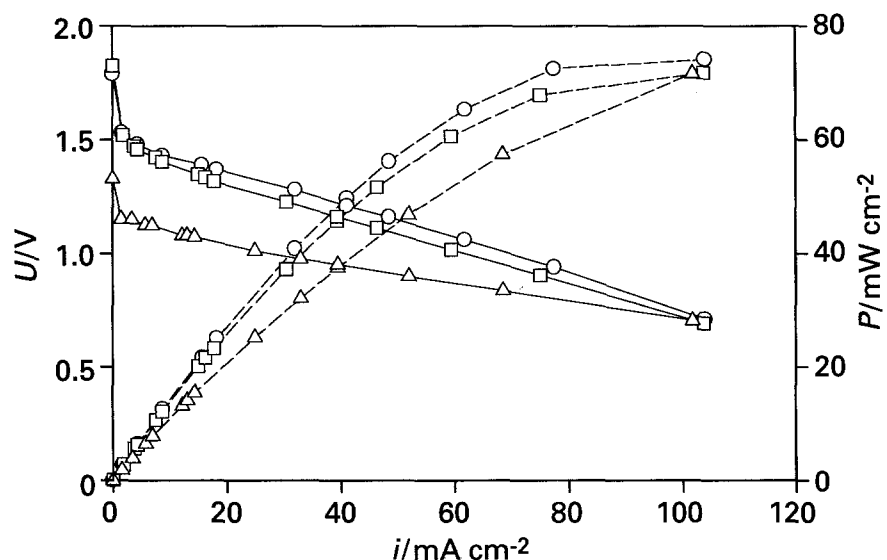


Fig. 4. Voltage (—) and power density (---) curves as functions of the current density obtained from a single cell with Al 99.99%. Electrolytes: (○) 7.5 M KOH, (□) 4 M NaOH, (△) 3 M H<sub>2</sub>SO<sub>4</sub> + 0.04 M HCl.

25° C was found to be  $0.386 \Omega^{-1} \text{ cm}^{-1}$  for 4 M NaOH,  $0.65 \Omega^{-1} \text{ cm}^{-1}$  for 7.5 M KOH, and  $0.8 \Omega^{-1} \text{ cm}^{-1}$  for 3 M H<sub>2</sub>SO<sub>4</sub>. 0.04 M HCl was added to the sulphuric acid in order to activate the aluminium electrode.

### 2.3. Apparatus

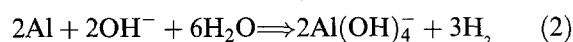
The current-potential curves were automatically recorded with an AT-PC 386. The data acquisition software was the Labtech Notebook 4.0. A series of different resistors was used to establish any given polarization curve. The external load was changed every 3 min with an electronic device built in house. The corresponding cell current, cell voltage and single electrode potentials measured against the reference electrode were recorded simultaneously every twenty seconds with a data acquisition board (RTI-815, Analog Device). In alkaline electrolytes, a Hg/HgO reference electrode filled with the same electrolyte as used in the battery was introduced between the anode and the cathode in order to measure the electrode potentials. A Hg/Hg<sub>2</sub>SO<sub>4</sub>/K<sub>2</sub>SO<sub>4</sub> sat. electrode was used in the acidic electrolyte. In all experiments a total amount of 400 ml electrolyte was used per cell compartment. The electrolyte reservoir was kept at 20° C.

### 3. Results and discussion

Figure 4 shows the voltage and the power density of a single cell with Al 99.99% measured as functions of the current density in three different electrolytes. These values, which were obtained with one series of external resistors, always represent the mean of nine measurements. An open-circuit voltage of 1.85 V was measured in the two alkaline electrolytes (KOH and NaOH) while in the acidic electrolyte (H<sub>2</sub>SO<sub>4</sub>) this value was 1.35 V. Between 0 and 10 mA cm<sup>-2</sup> there was a sharp, almost exponential decrease of the cell voltage, whereas at higher current densities the voltage decreased linearly with increasing current

density. From the slope of the linear part of the current-voltage curve, the internal resistance,  $r_{\text{int}}$ , of a single unit cell can be estimated. However,  $r_{\text{int}}$  is not inversely proportional to the conductivity of the electrolyte; its values reflect some contribution of the electron transfer resistance at the O<sub>2</sub> and Al electrode. A power of about  $75 \text{ mW cm}^{-2}$  was obtained at 0.7 V and a current density of  $103 \text{ mA cm}^{-2}$ . By optimizing the cell construction with smaller distances between the electrodes [23] and using alloys instead of pure aluminium, it was possible to boost the power density of the battery to  $160 \text{ mW cm}^{-2}$ .

The electrode polarization curves are shown in Fig. 5, where the electrode potentials are reported as functions of current density. At the aluminium electrode a mixed potential between the electrochemical oxidation of aluminium and the potential of hydrogen evolution is established at open circuit. In alkaline solutions this is based on the reactions described in Equations 1 and 2:



In sulfuric acid a thick aluminium oxide layer is formed and the electrochemical process is inhibited. However, when HCl is added to the sulfuric acid to obtain an electrolyte solution with 0.04 M HCl, local attack on the aluminium oxide layer results in pits. Within the pits electrochemical oxidation of aluminium and hydrogen production occur with the production of Al<sup>3+</sup> ions and subsequent formation of aqueous sulfate complexes. In alkaline and acidic solutions efficient electrochemical dissolution of aluminium is only observed at high overpotentials, e.g. at potentials that are more than 1 V more positive than the thermodynamic potential (-1.7 V vs RHE). This is due to a constantly renewed compact aluminium oxide layer with a thickness of less than 10 nm [24]. This oxide layer is a barrier for the electron transfer process.

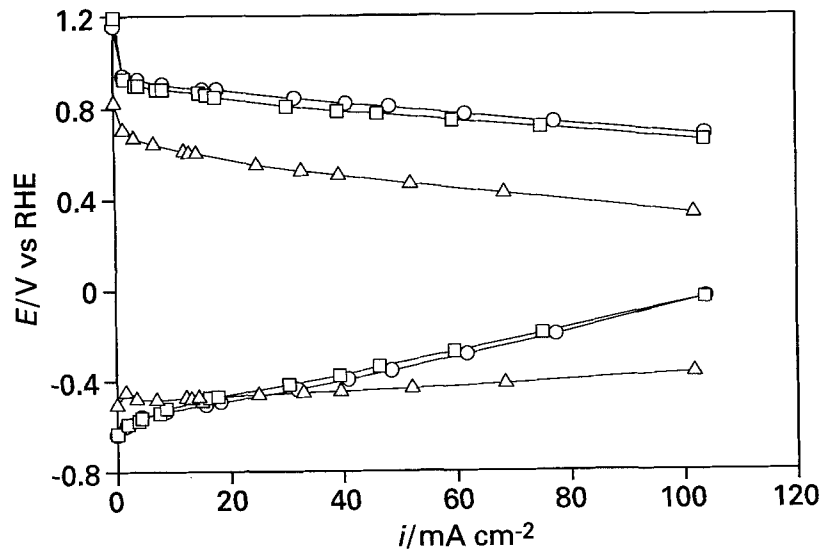


Fig. 5. Polarization curves of the Al 99.99% electrode and the oxygen electrode in three different electrolytes. Electrolytes: (○) 7.5 M KOH, (□) 4 M NaOH, (△) 3 M H<sub>2</sub>SO<sub>4</sub> + 0.04 M HCl.

In acidic electrolytes the anodic potential remains almost constant with increasing current density.

Oxygen reduction in KOH and NaOH occurs at considerably more positive potentials than in acidic solutions. This is a well known fact which is at least partly due to a change in the oxygen reduction mechanism [25]. In the present case the platinum catalyst is also poisoned by the HCl additive. Preliminary experiments showed that the oxygen electrode

potential in acidic solutions can be shifted by about 150 mV when pyrolysed Co-poly(chloranile amide) is used as the catalyst [26].

### 3.1. Alloys

The electrochemical dissolution of aluminium can be activated using special alloys. Fig. 6 shows the electrode polarization curves of three Al/O<sub>2</sub> batteries

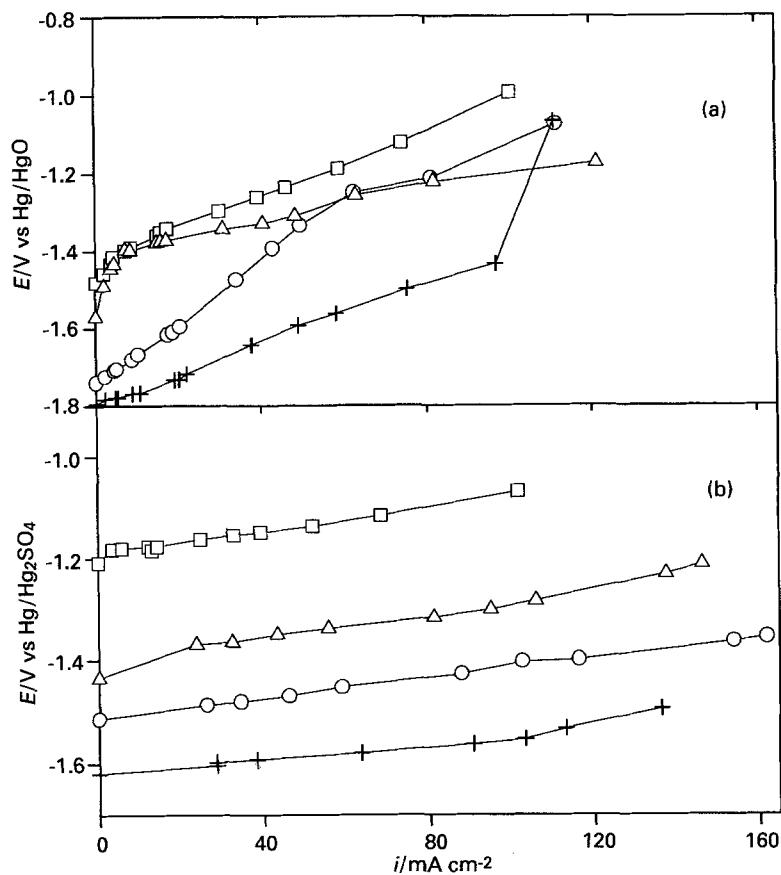


Fig. 6. (a) Polarization curves of three different Al alloys electrodes. Reference electrode Hg/HgO/4M NaOH. Electrolyte: 4 M NaOH. Aluminium composition: (□) Al 99.99% (+) Al-In0.05, (○) Al-Zn6.3 Sn0.16, (△) Al-In0.01 Zn 3.2. (b) Polarization curves of three different Al-alloys electrodes. Reference electrode: Hg/Hg<sub>2</sub>SO<sub>4</sub>/K<sub>2</sub>SO<sub>4</sub>. Electrolyte: 3 M H<sub>2</sub>SO<sub>4</sub> + 0.04 M HCl. Aluminium composition: (□) Al 99.99%, (+) Al-In0.10, (○) Al-Zn6.3 Sn0.16, (△) Al-In0.01 Zn3.2.

Table 1. Influence of aluminium alloy composition on the performance of the Al/O<sub>2</sub> battery in alkaline and acidic electrolytes

Electrolyte	Alloy*	OCP <sup>†</sup> /V vs Hg/HgO	$P_{\max}^{\ddagger}$ /mW cm <sup>-2</sup>
4 M NaOH	Al 99.99	-1.48	72
	Al-In	-1.79	120
	Al-Zn/Sn	-1.74	90
	Al-In/Zn	-1.57	110
7.5 M KOH	Al 99.99	-1.56	74
	Al-In	-1.82	160
	Al-Zn/Sn	-1.62	120
	Al-In/Zn	-1.59	100
OCP <sup>†</sup> /V vs Hg/Hg <sub>2</sub> SO <sub>4</sub>			
3 M H <sub>2</sub> SO <sub>4</sub> +	Al 99.99	-1.21	72
	Al-In	-1.62	110
0.04 M HCl	Al-Zn/Sn	-1.52	120
	Al-In/Zn	-1.44	100

\* Compositions are given in Section 2.2.

<sup>†</sup> Open circuit potential.

<sup>‡</sup> Maximum power density.

with different Al alloys measured in (a) alkaline (4 M NaOH) and (b) acidic (3 M H<sub>2</sub>SO<sub>4</sub> + 0.04 M HCl) electrolyte. A shift of the aluminium anode potential to values which are up to 400 mV closer to its thermodynamic potential was achieved in acidic solution using alloys containing Zn, Sn and In. In alkaline solution the potential shift for the same aluminium

alloys was between 30–300 mV (Table 1). Current-potential curves measured for aluminium in acidic electrolytes, and corrected for the electrolyte resistance, show a negative slope.

The activation mechanism in acidic electrolytes is not completely understood, but was already noticed by Despić *et al.* [27] and called a 'negative difference effect'. High current densities probably alter the structure of the oxide layer; the pits become larger in diameter, which lowers the resistance and thus the overpotential. The alloying elements lead to faster electrode kinetics due to modifications of the compact oxide layer [12, 13, 28, 29].

In alkaline electrolytes all three alloys exhibited a lower overpotential than pure aluminium. For the Al-In 0.05 alloy a sharp increase of the anodic potential were observed at high current densities. The same phenomenon was reported by Wilhelmson *et al.* [9] and was attributed to dissolution of indium at the surface and subsequent formation of an indium-free aluminium oxide layer.

The same experiments as reported in Fig. 6(a) and (b) were carried out in 7.5 M KOH. The results obtained are collected in Table 1. The highest power density (160 mW cm<sup>-2</sup>) was obtained with Al-In in 7.5 M KOH.

### 3.2. Bipolar configuration with two cells

With the bipolar cell arrangement represented in

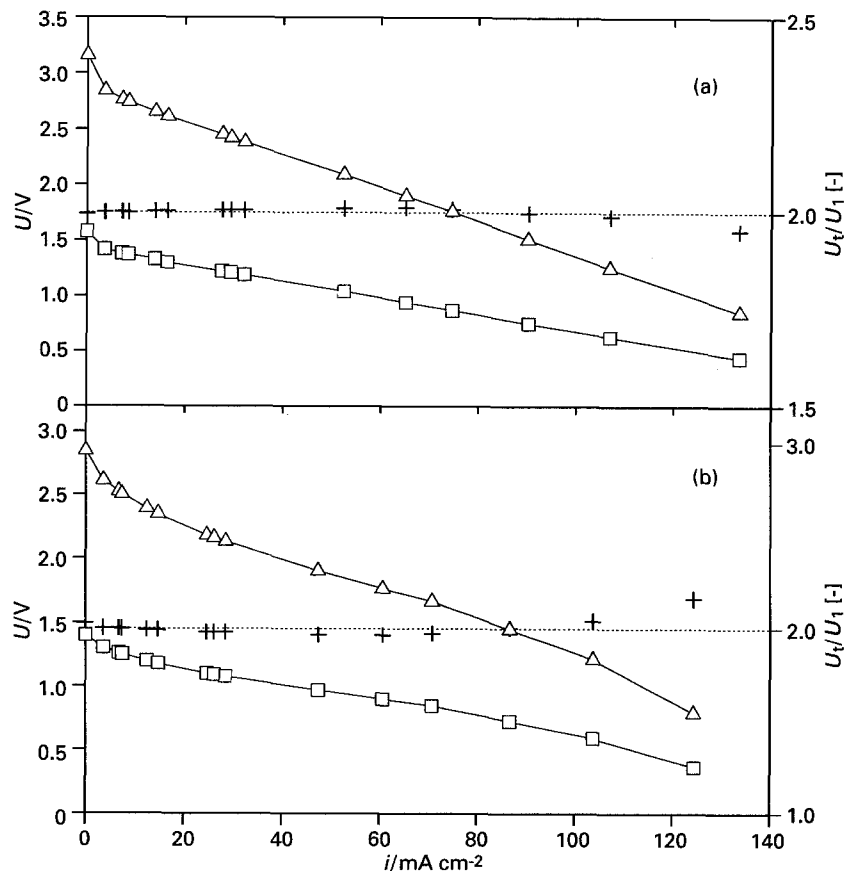


Fig. 7. Current-voltage curves of a bipolar Al/O<sub>2</sub> battery with two cells (as in Fig. 3.). Electrodes: Al 99.99% and Eltech oxygen electrode. ( $\Delta$ )  $U_t$  voltage at the terminals of the battery, ( $\square$ )  $U_1$  voltage of the first cell, (+)  $U_t/U_1$  ratio. Electrolytes: (a) 4 M NaOH, (b) 3 M H<sub>2</sub>SO<sub>4</sub> + 0.04 M HCl.

Table 2. Increase of the internal resistance with two cells

Electrolyte	$r_1^*$ / $\Omega \text{ cm}^2$	$r_t^\dagger$ / $\Omega \text{ cm}^2$	$r_t/r_1$
4 M NaOH	7.3	15.1	2.1
3 M H <sub>2</sub> SO <sub>4</sub> (+0.04 M HCl)	6.8	13.1	1.9

\*  $r_1$ : resistance of one element.

†  $r_t$ : total resistance.

Fig. 3, the cell voltage should be doubled for the same current density. The experimental data measured with a stack of two cells are depicted in Fig. 7(a) and (b). The experiments were carried out with pure aluminium (Al 99.99%) in alkaline (4 M NaOH: Fig. 7(a)) and in acidic electrolyte (3 M H<sub>2</sub>SO<sub>4</sub> + 0.04 M HCl: Fig. 7(b)). In each figure, the voltage of the battery  $U_t$ , the voltage of the first element  $U_1$  and the ratio between these two parameters were plotted as functions of the current density.

The experimental results are as expected. The voltage delivered by one cell represented almost one half of the global voltage at each current density. Only at current densities higher than 100 mA cm<sup>-2</sup> did the cell voltages start to deviate. No ohmic losses were evident, since the configuration adopted provides good electrical contact between the two electrodes of the bipolar element. The shunt current leakage which represents the most important limitation in bipolar configurations was avoided by feeding each compartment with its own electrolyte circuit

flowing through separate reservoirs. Both voltages,  $U_t$  and  $U_1$ , decreased almost linearly with increasing current density, and the corresponding total and partial resistance could be estimated from the slope (Table 2). The total resistance is the sum of the partial resistances placed in series. For high-power devices the internal resistance of each single cell should be minimized. With a smaller electrolyte gap, e.g. 2 mm, it would be possible to increase the power density by about 25%. This can be estimated from the reduced electrolyte resistance, which in our case contributes about 32% to the total internal resistance [30].

### 3.3. Bipolar configuration with four cells

The power output of bipolar batteries with four cells using Al 99.99% was measured as a function of the current density with 4 M NaOH (Fig. 8(a)) and 3 M H<sub>2</sub>SO<sub>4</sub> + 0.04 M HCl (Fig. 8(b)) as the electrolytes. The stack performance was close to that obtained with the one and two-cell arrangement. In alkaline electrolyte, the maximum power increased by 7.5 W for each additional cell. With four cells, a maximum power output of 30 W was obtained at 110 mA cm<sup>-2</sup> and a battery voltage of 2.7 V (0.675 V per cell). In acidic electrolytes an analogous behavior was observed, although the power increase achieved with each additional cell was less regular. With four cells, the power reached a maximum of 35 W at 170 mA cm<sup>-2</sup> and a battery voltage of 2 V (0.5 V per cell). As mentioned before, the power output in acidic

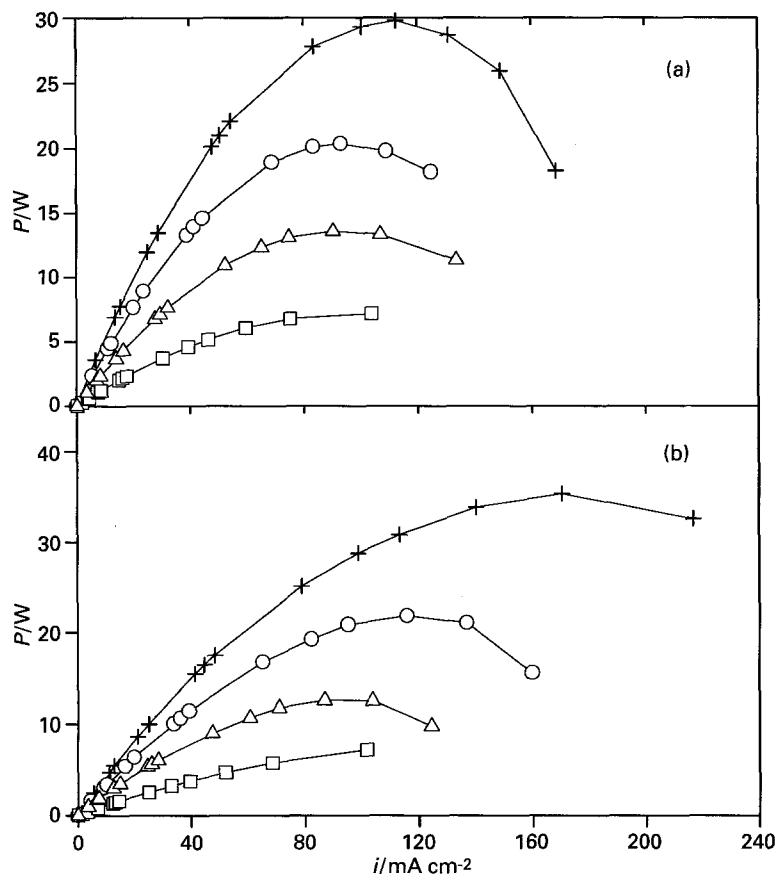


Fig. 8. Power output as function of the current density in a bipolar Al/O<sub>2</sub> stack with one to four cells. Electrodes: Al 99.99% and Eltech oxygen electrode. (□) 1 cell, (△) 2 cells, (○) 3 cells, (+) 4 cells. Electrolytes: (a) 4 M NaOH, (b) 3 M H<sub>2</sub>SO<sub>4</sub> + 0.04 M HCl.

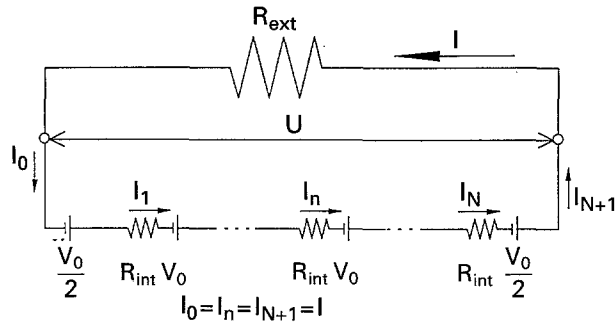


Fig. 9. Equivalent circuit of a bipolar Al/O<sub>2</sub> battery containing  $N$  cells. Each unit cell is represented as an ideal voltage source  $V_0$  with an internal resistance  $R_{int}$  in series.

electrolytes could be increased considerably if adequate alloys and Pt-free catalysts were used [13]. As expected, with a larger number of cells in the battery, the maximum power is reached at correspondingly higher external loads.

### 3.4. Equivalent circuit

The bipolar stack can be described by an equivalent circuit as depicted in Fig. 9 [31]. Each cell is represented as an ideal voltage source,  $V_0$ , in series with an internal resistance,  $R_{int}$ , where  $V_0$  is obtained by extrapolating the linear part of the current-potential curve to  $I = 0$ . This assumption implies that the polarization characteristic of each cell is linear, which is a good approximation according to the polarization curves in Fig. 4. As the electrolyte flows are com-

pletely separated, the current bypass is not taken into account. Application of Kirchhoff's laws to this circuit results in a summation of the potential drops around the loop formed by  $N$  cells and the external load:

$$U = R_{ext}I = NV_0 - NR_{int}I \quad (3)$$

$$I = \frac{NV_0}{R_{ext} + NR_{int}} \quad (4)$$

The power delivered as a function of the experimental parameter  $R_{ext}$  is calculated by Expression 5:

$$P = I^2 R_{ext} = [NV_0 / (R_{ext} + NR_{int})]^2 R_{ext} \quad (5)$$

The power maximum is reached at  $\partial P / \partial R_{ext} = 0$ , which leads to

$$R_{ext} = NR_{int} \quad (6)$$

and

$$P_{max} = \frac{NV_0^2}{4R_{int}} \quad (7)$$

$$I_{max} = \frac{V_0}{2R_{int}} \quad (8)$$

The maximum power and current output,  $P_{max}$  and  $I_{max}$ , can therefore be estimated from Relations 7 and 8. Both parameters are inversely proportional to the internal resistance of the unit cell. Relation 8 shows that the current at which the maximum power output occurs should not depend on the number of elements in the battery. The experiments, however, show a shift of the power maximum to higher current

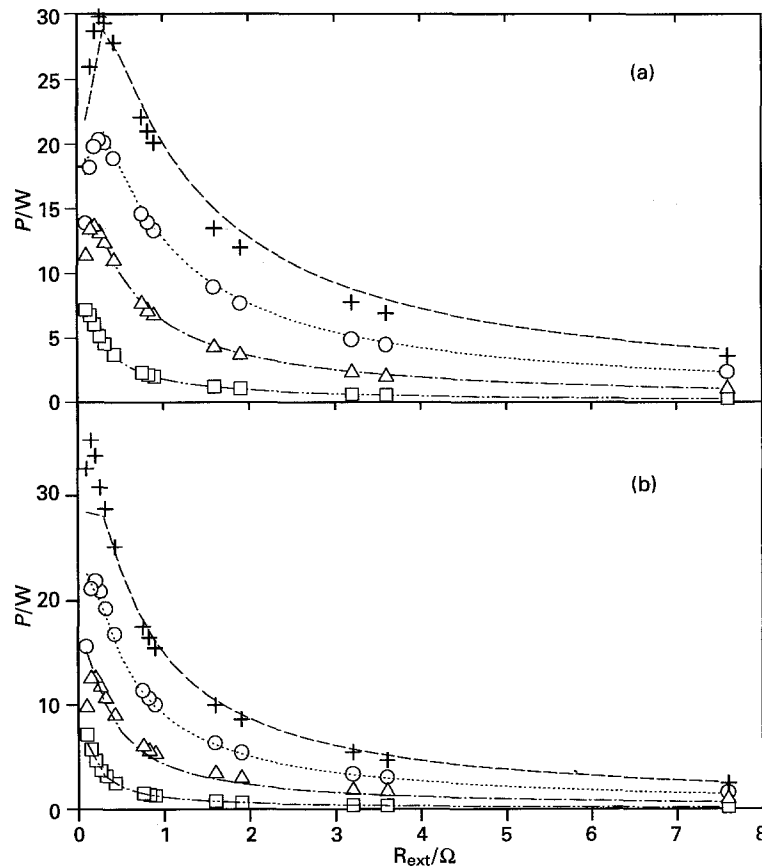


Fig. 10. Power output of the bipolar cell arrangement as a function of the external load, ( $\square$ ) 1 cell, ( $\triangle$ ) 2 cells, ( $\circ$ ) 3 cells, (+) 4 cells. Electrolytes: (a) 4M NaOH, (b) 3M H<sub>2</sub>SO<sub>4</sub> + 0.04M HCl. Lines represent calculated values from Equation 5.

Table 3

Electrolyte	V <sub>0</sub> /V	R <sub>int</sub> /Ω
NaOH 4 M	1.45	0.073
H <sub>2</sub> SO <sub>4</sub> 3 M (+0.04 M HCl)	1.13	0.042

densities with increasing cell number, especially when acidic electrolytes are used. This is not expected from the model, but may be explained by uncertainties arising from small differences in the cells used for the experiments. However, the validity of the model is demonstrated in Fig. 10(a) and (b) for external resistances higher than 0.3 Ω. According to the polarization curves reported in Fig. 4, the experimental parameters reported in Table 3 could be used to simulate the behaviour of the cell stack.

The power output is presented in these two figures as a function of the external load R<sub>ext</sub>. It can be seen that the behaviour of a bipolar Al/O<sub>2</sub> stack can be satisfactorily predicted from the measured internal resistance and the extrapolated open-circuit voltage of a single cell.

#### 4. Conclusions

The feasibility of a bipolar Al/O<sub>2</sub> battery with planar 100 cm<sup>2</sup> electrodes has been demonstrated using stacks with up to four cells. The performance of single cells was tested in alkaline (4 M NaOH, 7.5 M KOH) and acidic (3 M H<sub>2</sub>SO<sub>4</sub> + 0.04 M HCl) electrolytes. For a single cell, typical power densities of about 75 mW cm<sup>-2</sup> at 0.7 V were obtained with pure aluminium and 10 mm electrode distance. Further improvements can be achieved using alloys with elements like Zn, Sn and In. With these alloys, power densities of up to 120 mW cm<sup>-2</sup> in 4 M NaOH and 160 mW cm<sup>-2</sup> in 7.5 M KOH were reached. With acidic electrolytes the electrolyte resistance is lower and, in principle, even higher power densities are possible. The results obtained with two, three and four bipolar cells indicated the expected behaviour of the stack. Over the whole range of current densities, the voltage output of each individual cell was very similar.

Considerable improvements of the stack performance is possible when appropriate alloys and lower electrode distances are used. For further scale-up the heat removal may become a major problem. Due to its high energy density, the most interesting application of the Al/air battery could be as a power supplier in the telecommunication field in remote regions.

#### Acknowledgement

This work was supported by the Nationaler Energie-Forschungs-Fonds (NEFF-Projekt 382). We thank

Dr K. Müller from Battelle Research Centres in Geneva for comments on the manuscript.

#### References

- [1] S. Zaromb, *J. Electrochem. Soc.* **109** (1962) 1125.
- [2] A. R. Despic, 'The Use of Aluminium in Energy Conversion and Storage', in Proceedings of the first European East-West Workshop on Chemistry and Energy, Sintra, Portugal (1990) p. 143.
- [3] J. F. Cooper, K. A. Kraftick and B. J. McKinley, 'Current Status of the Development of the Refuelable Aluminium-Air Battery', in Proceedings of 18th Intersociety Energy Conversion Engineering Conference, Paper 839 266, Orlando FL (1993) p. 1628.
- [4] G. M. Scamans, W. B. O'Callaghan, N. P. Fitzpatrick and R. P. Hamlen, in Proceedings of 21st Intersociety Energy Conversion Engineering Conference, San Diego CA (1986) p. 1057.
- [5] D. D. Macdonald and C. English, *J. Appl. Electrochem.* **20** (1990) 405.
- [6] D. Macdonald, S. Real and M. Urquidi-MacDonald, *J. Electrochem. Soc.* **135** (1988) 2397.
- [7] D. Macdonald, S. Real, S. I. Smedley and M. Urquidi-MacDonald, *ibid.* **135** (1988) 2410.
- [8] S. Real, M. Urquidi-MacDonald and D. Macdonald, *ibid.* **135** (1988) 1633.
- [9] W. Wilhelmsen, T. Arnesen, O. Hasvold and N.J. Storkersen, *Electrochim. Acta* **36** (1991) 79.
- [10] C. D. S. Tuck, J. A. Hunter and G. M. Scamans, *J. Electrochem. Soc.* **134** (1987) 2970.
- [11] A. R. Despic, D. M. Drazic, M. M. Purenovic and N. Cikovic, *J. Appl. Electrochem.* **6** (1976) 527.
- [12] D. M. Drazic, A. R. Despic and S. Zecevic, 'Anodic Behavior of Al and the Alloys Al-In and Al-In-Ga in Aluminium-Air Batteries, UCRL-Trans-11534, Lawrence Livermore Laboratory Library, Livermore, Nov. (1979).
- [13] F. Holzer, S. Müller, J. Desilvestro and O. Haas, *J. Appl. Electrochem.* **23** (1993) 125.
- [14] L. A. Knerr and D. J. Wheeler, 'Aluminium-Air Battery Development', Final Report, UCRL-15686, Lawrence Livermore Laboratory (1985).
- [15] A. Maimoni, 'Aluminium-Air Battery Crystallizer', UCRL 95923, Lawrence Livermore National Laboratory, Jan. (1987).
- [16] M. Katoh, K. Shimizu and S. Katoh, *Denki Kagaku* **38** (1970) 753.
- [17] D. J. Levy, R. P. Hollandsworth, E. M. Gonzales and E. L. Littauer, 'Performance of a Rapidly-Refuelable Aluminium-Air Battery', in Proceedings of 18th Intersociety Energy Conversion Engineering Conference, Paper 839 267, Orlando FL (1983) p. 1635.
- [18] E. Budevski, I. Iliev, A. Kaisheva, A. Despic and K. Krsmanovic, *J. Appl. Electrochem.* **19** (1989) 323.
- [19] O. Hasvold, *Chem. and Ind.* (1988) 85.
- [20] A. R. Despic, *J. Appl. Electrochem.* **15** (1985) 191.
- [21] M. J. Niksa and D. J. Wheeler, *J. Power Sources* **22** (1988) 261.
- [22] P. A. Wycliffe, US Patent 4988 581 (1991).
- [23] S. Müller, F. Holzer, O. Haas, M. Rota, C. Cominellis, Ext. Abstract. ISE-Mecting, Montreux, 25-30 Aug. (1991).
- [24] B. Schnyder, R. Kötz, *J. Electroanal. Chem.* **339** (1992) 167.
- [25] K. Kinoshita, in 'Carbon: Electrochemical and Physicochemical Properties', Wiley Interscience (1988) p. 360.
- [26] Th. Allmendinger, PhD thesis nr. 9910 ETH, Zurich (1992).
- [27] A. R. Despic, D. M. Drazic, M. M. Purenovic and N. Cikovic, *J. Appl. Electrochem.* **6** (1976) 527.
- [28] G. Buri, W. Ludi and O. Haas, *ibid.* **136** (1989) 2167.
- [29] J. F. Equey, S. Müller, J. Desilvestro and O. Haas, *ibid.* **139** (1992) 1499.
- [30] M. Rota, PhD thesis nr. 1139 EPF, Lausanne (1993).
- [31] E. A. Kaminski and R. F. Savinell, *J. Electrochem. Soc.* **130** (1983) 1103.